

We are IntechOpen, the world's leading publisher of Open Access books Built by scientists, for scientists

6,600

Open access books available

178,000

International authors and editors

195M

Downloads

Our authors are among the

154

Countries delivered to

TOP 1%

most cited scientists

12.2%

Contributors from top 500 universities



WEB OF SCIENCE™

Selection of our books indexed in the Book Citation Index
in Web of Science™ Core Collection (BKCI)

Interested in publishing with us?
Contact book.department@intechopen.com

Numbers displayed above are based on latest data collected.
For more information visit www.intechopen.com



Chapter

Diffusion Magnetic Resonance Imaging (MRI)-Biomarkers for Diagnosis of Parkinson's Disease

Gloria Cruz, Shengdong Nie and Juan Ramírez

Abstract

Parkinson's disease (PD) is a degenerative neurological disorder, the origin of which remains unclear. The efficacy of treatments is limited due to the small number of remaining neurons. Diffusion magnetic resonance imaging (MRI) has revolutionized clinical neuroimaging. This noninvasive and quantitative method gathers *in vivo* microstructural information to characterize pathological processes that modify nervous tissue integrity. The changes in signal intensity result from the motion of the water molecules; they can be quantified by diffusivity measures. Diffusion MRI has revealed "biomarkers" in several brain regions that could be useful for PD diagnosis. These regions include the olfactory tracts, putamen, white matter, superior cerebellar peduncles, middle cerebellar peduncle, pons, cerebellum, and substantia nigra. There are encouraging preliminary data that differentiate PD from atypical parkinsonian diseases based on these microstructural changes.

Keywords: brain imaging, Parkinson's disease, diffusion MRI, atypical parkinsonian diseases, neuroimaging

1. Introduction

Parkinson's disease (PD) was first described in 1817 by James Parkinson and is characterized by the selective loss of dopaminergic neurons in the substantia nigra pars compacta (SNpc) [1–3]. Although PD has been known for more than two centuries, its origin remains unclear. The motor symptoms in patients with PD appear when at least 50–80% of dopaminergic neurons have been lost in the substantia nigra (SN). For this reason the quantity of remaining neurons limits the efficacy of treatments. PD begins with a reduction in dopamine signaling from the SN to the basal ganglia, which causes a decrease in the neuronal excitation localized in the thalamus. This abnormal condition is reflected by the symptoms of bradykinesia (slow or difficult movements), rigidity, postural instability, resting tremor, and non-motor symptoms in conjunction with fatigue, reduced facial expressions, sleep and smell disturbances, depression, and cognitive decline [4].

Conventional magnetic resonance imaging (MRI) does not provide adequate contrast to study changes in the brain of patients with PD. Indeed, conventional 1.5 T T1-

and T2-weighted sequences do not collect information for the SNpc. Hence, conventional MRI cannot detect structural lesions that cause PD and cannot differentiate PD from characteristic alterations of atypical parkinsonism diseases (APD), such as multiple system atrophy (MSA) and progressive supranuclear palsy (PSP). Conventional MRI neuroimaging is not specifically recommended for routine diagnosis in clinical practice of the difficulty in PD [5].

Diffusion MRI is an evolution of conventional MRI and has the potential to differentiate between PD and APD. This ability includes identifying the principal changes in the SN and the lower part of the putamen/caudate complex, the location of most nigrostriatal dopaminergic neurons. Changes in these areas in patients with PD could provide valuable information to aid in the diagnosis and assess disease progression. Diffusion MRI involves two techniques: (1) diffusion-weighted imaging (DWI) shows the change in a particular water molecule diffusing from one location to another over a given period of time estimated by the apparent diffusion coefficient (ADC). (2) Diffusion tensor imaging (DTI) is a useful method to measure the directionality of water inside living systems, which is estimated by fractional anisotropy (FA). The fundamental aims of the use of diffusion MRI in PD are: (1) to contribute to the differential clinical diagnosis between PD and APD; (2) to determine biomarkers of disease progression and, therefore, to demonstrate the usefulness of potential therapies that delay or improve disease progression; (3) to allow presymptomatic diagnosis in people with PD; and (4) to identify in advance the motor and non-motor complications.

This chapter reviews the available data on the use of diffusion MRI to determine the pathophysiological mechanisms responsible for PD and APD. This technique could be used to identify microstructural changes earlier and thus initiate treatment more quickly after PD onset. It also offers the potential to differentiate between PD and APD.

2. Basic of diffusion

Diffusion is the physical property that describes the Brownian (random) movement of water molecules in biological tissue in response to thermal energy [5]. The human body is composed of 75% water, which is located in three compartments: intravascular, intracellular, and extracellular (**Figure 1**). The movement of water molecules at the microscopic level of these compartments is sensitive to the diffusion sequence. Of note, it is the movement of water molecules in the extracellular space that is most useful to identify quantifiable markers that reflect tissue alterations. Microscopic displacement of water molecules occurs within brain tissue by following diffusion [7, 8]. Identifying these alterations in these movements could be useful to characterize neurodegenerative diseases, such as PD.

In 1965, Stejskal and Tanner [9] were the first to apply the property of diffusion to MR sequences. In 1980, researchers reported the first biological tissues imaged based on the principles of nuclear magnetic resonance established by Carr et al. [10]. In 1986, Le Bihan et al. developed the first diffusion image from a brain MRI [11]. In 1992, Warach et al. [12] first applied this technique to study cerebral infarction. An advantage of this technique is its noninvasive nature and it does not require ionizing radiation and paramagnetic contrast. There is a great interest in MRI use to measure water diffusion. This application could provide maps of the diffusion coefficients in tissues, particularly *in vivo* [7]. Identifying areas of interest could be useful in defining biomarkers that could improve the diagnosis or traceability of a specific pathology.

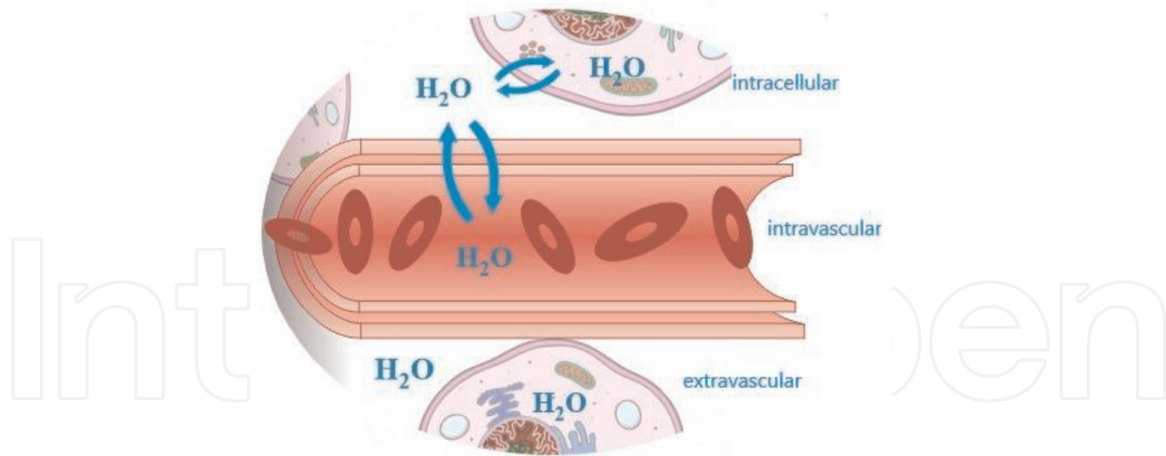


Figure 1.
 A model of biological tissue described by three compartments: extravascular, intravascular, and intracellular. In healthy brain, water (H_2O , which forms the basis for the magnetic resonance signal) is present and exchanged among all three compartments. This figure is based on the model from Anderson et al. [6].

2.1 Brief background of diffusion MRI

Diffusion MRI, also known as DWI, is a procedure of MRI based upon measuring the motion of water molecules within a voxel of biological tissue. Diffusion MRI detected the Brownian motion that is observed in the random or uncontrolled movement of particles in a fluid as they constantly collide with other molecules [13]. The pulsed gradient spin echo sequence, shown in **Figure 2**, is the most used acquisition scheme to generate diffusion weighting in an MRI image. It is also widely used to measure the displacement of water molecules in tissue. It consists of two radio-frequency (RF) pulses, one at 90° and the second at 180° , and two magnetic gradients with intensity G and pulse duration δ , before and after the 180° RF pulse.

In the MRI literature, the sequence parameters (see **Figure 2**) are commonly represented by a single diffusion parameter, b . It can be calculated according to Eq. (1):

$$b = \gamma^2 G^2 \delta^2 \left(\Delta - \frac{\delta}{3} \right). \quad (1)$$

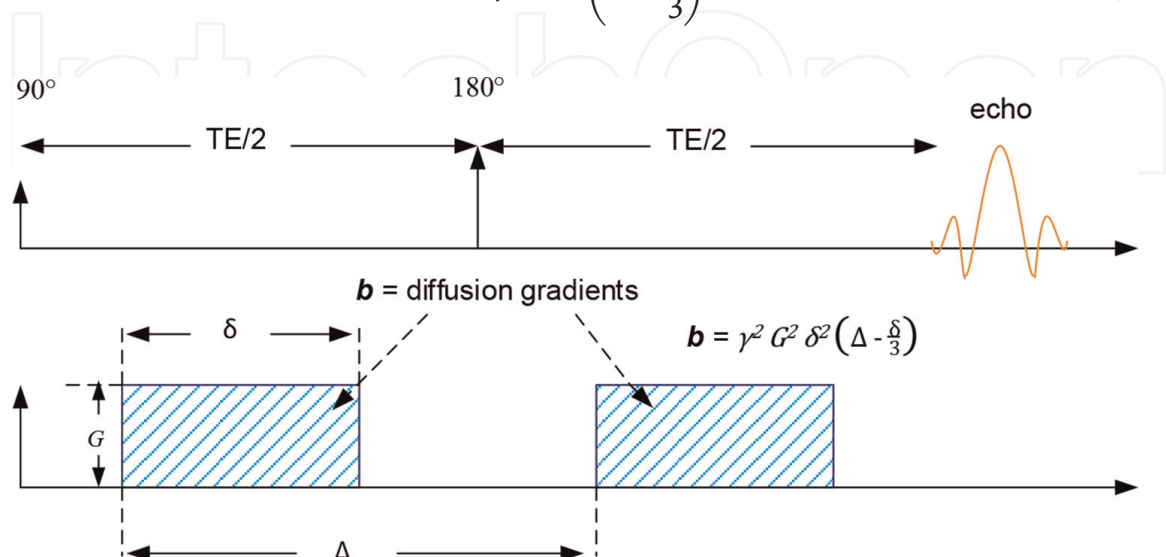


Figure 2.
 The Stejskal-Tanner pulsed-gradient spin echo (PGSE) sequence [9]. δ is the pulse duration, G is the pulse gradient, Δ is the diffusion time and echo time (TE) is the time to echo [14, 15].

Diffusion MRI quantifies the motion of water molecules (see **Table 1**). Microstructural changes in neuronal tissue are determined by quantifying the diffusion coefficients, measured by applying a diffusion-sensitizing gradient using the isotropic signal decay formulated by Stejskal-Tanner, which is called the apparent diffusion coefficient (ADC). This measure allows for evaluating the average diffusion in the area of interest of a tissue. Isotropic diffusion refers to the lack of a preferred direction for diffusion. An example is cerebrospinal fluid in which the diffusion rate of molecules is equal in all directions [16, 17]. The ADC map is created with the mono-exponential model by applying a square noise filter to define the intensity scale based on b -values (**Figure 3**).

DTI was first described by Basser et al. [18]. It provides information about the local tissue when diffusion depends on the direction and is restricted by the normal architecture of the brain and the neuronal tracts, a condition known as anisotropy. Hence, DTI allows for calculating fractional anisotropy (FA) [19]. Anisotropic diffusion is not equal in all directions. An example is diffusion in neural tracts, where water molecules diffuse more longitudinally along the tract than to the sides. This directionality is largely determined by the cellularity and cell integrity in the tissues [16, 17]. FA is an important measure to detect any structural change with respect to a direction defined by the neuronal tissue. DTI is a sensitive, noninvasive method to detect the early stages of PD [20]. It even differentiates microstructural changes in PD (**Figures 4 and 5**) [21].

Diffusion imaging	Measures	Details
Diffusion-weighted imaging	Apparent diffusion coefficient (ADC), or trace (D) diffusion coefficient is a measure of the strength (velocity) of diffusion in tissue.	Isotropic diffusion are called the distance to travel by the water molecules in the tissue, without barriers that restrict and the move nor the direction.
Diffusion tensor imaging	Fractional anisotropy	The molecules are limited to a determined direction of the tissue, generating a tensor that has three diffusion components on each axis (x, y, and z).

Table 1.
Diffusion MRI techniques.

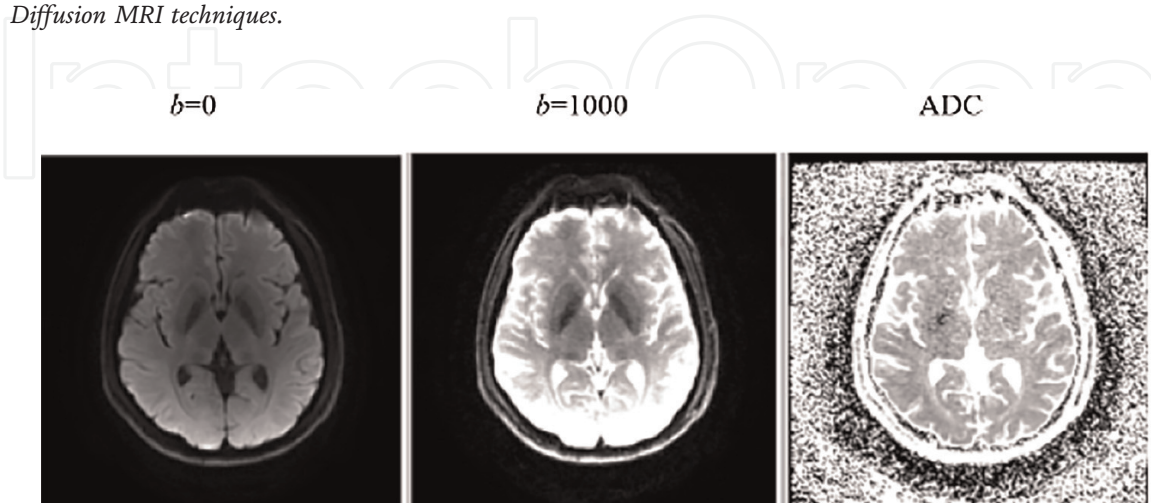


Figure 3.
PD-DWI images use two different b -values, 43-year-old patient PD, male. Apparent diffusion coefficient (ADC) maps created from the linear representation of the mono-exponential model in patients with Parkinson's disease. The signal obtained with the b -value provides information about the diffusion constant (made by the authors).

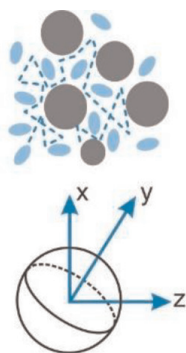


Figure 4. Random barriers are present. Information on the microscopic motion of water protons (made by the authors).

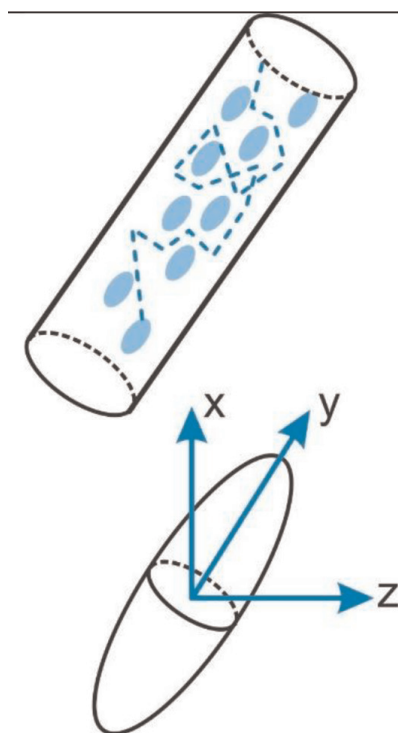


Figure 5. Coherent axonal bundle. Information on diffusion directionality, for example, it is possible to reconstruct axonal or muscle fiber images (made by the authors).

3. Diagnosis of PD and APD

PD and APD are characterized by progressive dopaminergic dysfunction. Diagnosis and treatment of diseases in their early stages can be complicated [20]. While conventional MRI has provided information on these diseases (**Table 2**), diffusion MRI can help to provide additional information and specific biomarkers to help distinguish among them (**Figures 6–8**) [29].

3.1 Diffusional MRI findings in PD

DWI and DTI provide quantifiable information to detect microstructural changes in PD. Neuronal loss alters the structural architecture of the central nervous system, producing potential biomarkers that could be assessed with imaging to diagnose PD (**Table 3**) (**Figures 9–20**) [28, 29, 32, 51–53].

Definition	Affected areas	Typical imaging findings
MSA including MSA-P and MSA-C [22]	The putamen and cerebellum are both affected in MSA, and nigral dopaminergic neuronal loss is observed in both MSA and PD [23]. Increased putaminal diffusivity in a patients with MSA. ADC is increased in the area of the lenticular nucleus in the patient with MSA [24].	
PSP is characterized by postural instability and supranuclear gaze palsy; it is sometimes called Richardson's syndrome [25]	Pathological changes in the SCP and dentate nucleus. Extensive atrophy in the brain stem, particularly in the midbrain, and also in the basal ganglia and cortex [24]	
CBS includes apraxia, the alien-limb phenomenon, and disturbed epicritic sensitivity [26]	The most common motor feature in CBS is asymmetrical parkinsonism affecting a limb, typically an arm.	

Abbreviations: ADC: apparent diffusion coefficient; CBS: corticobasal syndrome; FLAIR: fluid-attenuated inversion recovery; MSA: multiple system atrophy; MSA-C: multiple system atrophy with predominant cerebellar dysfunction; MSA-P: multiple system atrophy with predominant parkinsonian features; PD: Parkinson's disease; PSP: Progressive supranuclear palsy; SCP: superior cerebellar peduncle.

Table 2.
The main diagnosis of parkinsonian diseases.

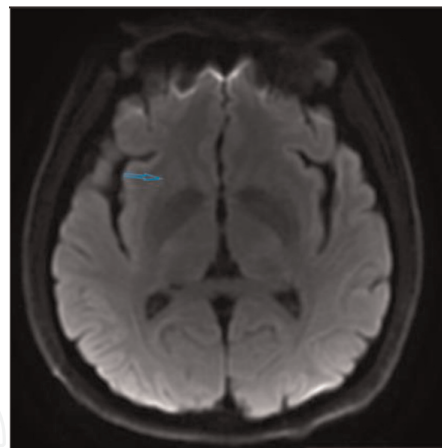


Figure 6.
The area of the lenticular nucleus 43-year-old patient PD, male (made by the authors).

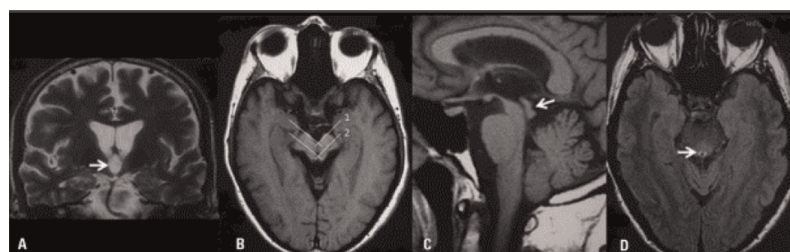


Figure 7.
DWI images of a patient with PSP. (A) Enlargement of the third ventricle (B). Internal-1 and external-2 interpeduncular angles show midbrain atrophy. (C) Quadrigeminal thickness showing atrophy. (D) Periaqueductal hypersignal. Adapted from Barsottini et al. [27].

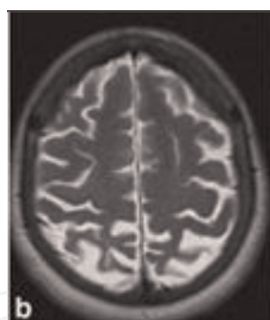


Figure 8. Corticobasal degeneration. T2-weighted spin echo (b) demonstrates thinning of the sulci in the parietal cortex combined with subtle hyperintensity of the subcortical white matter. Adapted from Mascaldi et al. [28].

Technique and region	Diffusion MRI findings	Key diffusion measures	Reference
DWI in olfactory tracts	Patients with PD showed significant increases in trace of diffusion (D) values in both olfactory tracts in a cohort of patients with PD versus healthy controls. Adapted from Ref. [30].	Patients with PD Trace (D) $>0.78 \times 10^{-3} \text{ mm}^2/\text{s}$ Healthy controls Trace (D) $<0.78 \times 10^{-3} \text{ mm}^2/\text{s}$	[30]
DTI to show olfactory dysfunction	Understanding the neurological substrates of olfactory dysfunction in early PD could be used in combination with clinical markers. Identify evidence of white matter areas with increased/decreased connectivity in patients with PD with complete or severe loss of olfaction.		[31]
DWI of the putamen	PD, MSA-P, and healthy controls marked differences in putaminal ADC maps among patients. Putaminal ROIs denote descending regional ADC values. Adapted from Ref. [32].	Putaminal regional ADC Patients with MSA-P ADC median = $0.791 \times 10^{-3} \text{ mm}^2/\text{s}$ Patients with PD ADC median = $0.698 \times 10^{-3} \text{ mm}^2/\text{s}$ Healthy controls ADC median = $0.727 \times 10^{-3} \text{ mm}^2/\text{s}$	[32]
DTI of the putamen	Schocke et al. [33] provided trace (D) imaging, which appears to be more accurate to separate patients with MSA-P from patients with PD, as rADC values in one direction are dependent on the slice orientation relative to the directions of fiber tracts. The ADC maps in the y-direction and z-direction clearly show the bilateral putaminal hyperintensity in	Putamen Increased putaminal diffusivity: rADC in the y- and z-direction as well as trace (D) clearly show bilateral putaminal hyperintensity. Patients with MSA-P rADC in the y-direction = $1.011 \pm 0.196 \times 10^{-3} \text{ mm}^2/\text{s}$ rADC in the x-direction = $0.750 \pm 0.180 \times 10^{-3} \text{ mm}^2/\text{s}$ Trace (D) = $0.926 \pm 0.208 \times 10^{-3} \text{ mm}^2/\text{s}$ Patients with PD rADC in the y-direction = $0.766 \pm 0.036 \times 10^{-3} \text{ mm}^2/\text{s}$	[33]

Technique and region	Diffusion MRI findings	Key diffusion measures	Reference
	a patient with MSA, indicating increased putaminal rADCs and rTrace (D) values. The putaminal hyperintensity is poorly demarcated on the ADC map in the x-direction.	rADC in the x-direction = $0.591 \pm 0.0058 \times 10^{-3} \text{ mm}^2/\text{s}$ Trace (D) = $0.718 \pm 0.030 \times 10^{-3} \text{ mm}^2/\text{s}$ Healthy controls rADC in the y-direction = $0.769 \pm 0.025 \times 10^{-3} \text{ mm}^2/\text{s}$ rADC in the x-direction = $0.637 \pm 0.071 \times 10^{-3} \text{ mm}^2/\text{s}$ Trace (D) = $0.745 \pm 0.024 \times 10^{-3} \text{ mm}^2/\text{s}$	
DTI of white matter	Significant differences between patients with MSA-P and patients with PD.	White matter Patients with MSA-P rADC in the y-direction = $0.833 \pm 0.067 \times 10^{-3} \text{ mm}^2/\text{s}$ ($P = 0.004$) Patients with PD rADC in the y-direction = $0.769 \pm 0.052 \times 10^{-3} \text{ mm}^2/\text{s}$ ($P = 0.004$) Healthy controls rADC in the y-direction = $0.733 \pm 0.039 \times 10^{-3} \text{ mm}^2/\text{s}$ ($P = 0.004$)	[33]
DTI of the caudate nucleus	Significant differences in trace (D) of the caudate nucleus between patients with MSA-P and patients with PD. The caudate nucleus also shows significant differences in the rADC in the y-direction between patients with MSA-P or PD and healthy controls.	Caudate nucleus Patients with PD Trace (D) = $0.725 \pm 0.035 \times 10^{-3} \text{ mm}^2/\text{s}$ Patients with MSA-P Trace (D) = $0.802 \pm 0.125 \times 10^{-3} \text{ mm}^2/\text{s}$ Patients with PD rADC in y-direction = $0.808 \pm 0.043 \times 10^{-3} \text{ mm}^2/\text{s}$ Patients with MSA-P rADC in y-direction = $0.914 \pm 0.120 \times 10^{-3} \text{ mm}^2/\text{s}$ Healthy controls rADC in y-direction = $0.823 \pm 0.051 \times 10^{-3} \text{ mm}^2/\text{s}$	[33]
DTI of the globus pallidus	Significant differences: 1. rADC between patients with MSA-P or PD patients and healthy controls for the z- and x-directions. 2. Trace (D) between patients with MSA-P or PD and healthy controls.	Globus pallidus Patients with MSA-P rADC in the z-direction = $0.829 \pm 0.109 \times 10^{-3} \text{ mm}^2/\text{s}$ Patients with PD rADC in the z-direction = $0.737 \pm 0.049 \times 10^{-3} \text{ mm}^2/\text{s}$ Healthy controls rADC in the z-direction = $0.798 \pm 0.068 \times 10^{-3} \text{ mm}^2/\text{s}$ Patients with MSA-P rADC in the x-direction = $0.879 \pm 0.120 \times 10^{-3} \text{ mm}^2/\text{s}$ Patients with PD rADC in the x-direction = $0.736 \pm 0.108 \times 10^{-3} \text{ mm}^2/\text{s}$	[33]

Technique and region	Diffusion MRI findings	Key diffusion measures	Reference
		Healthy controls rADC in the x-direction = 0.721 $\pm 0.092 \times 10^{-3} \text{ mm}^2/\text{s}$ Patients with MSA-P Trace (D) = 0.802 $\pm 0.125 \times 10^{-3} \text{ mm}^2/\text{s}$ Patients with PD Trace (D) = 0.725 $\pm 0.035 \times 10^{-3} \text{ mm}^2/\text{s}$ Healthy controls Trace (D) = 0.747 $\pm 0.034 \times 10^{-3} \text{ mm}^2/\text{s}$	
DWI of the SCP ADC differentiates between patients with PSP and patients with PD		SCP Patients with PSP Median rADC = $0.98 \times 10^{-3} \text{ mm}^2/\text{s}$ Patients with MSA-P Median rADC = $0.79 \times 10^{-3} \text{ mm}^2/\text{s}$ ($P < 0.001$) Patients with PD Median rADC = $0.79 \times 10^{-3} \text{ mm}^2/\text{s}$ ($P < 0.001$) Healthy controls Median rADC = $0.80 \times 10^{-3} \text{ mm}^2/\text{s}$ ($P < 0.001$)	[34, 35]
DTI of the putamen in patients with MSA-P	Putaminal trace (D) in patients with MSA-P has been mapped at the level of the mid-striatum. The diffuse hyperintensity corresponding to increased trace (D) in the putaminal region of the patient with MSA [36].	The patient with MSA Putamen Trace (D) $> 0.80 \times 10^{-3} \text{ mm}^2/\text{s}$ Posterior putamen Trace (D) $> 0.80 \times 10^{-3} \text{ mm}^2/\text{s}$	[37]
DWI of the middle cerebellar peduncle to differentiate between patients with MSA-P, PSP or PD	Increased middle cerebellar peduncle rADC. The images show patients with MSA without cruciform hyperintensity and patients with MSA with cruciform hyperintensity [37].	Increased middle cerebellar peduncle rADC differentiates patients with MSA-P from patients with PSP and PD. Patients with MSA-P Median rADC = $0.93 \times 10^{-3} \text{ mm}^2/\text{s}$ ($P < 0.001$) Patients with PSP Median rADC = $0.82 \times 10^{-3} \text{ mm}^2/\text{s}$ Patients with PD Median rADC = $0.79 \times 10^{-3} \text{ mm}^2/\text{s}$ ($P < 0.001$) Healthy controls Median rADC = $0.81 \times 10^{-3} \text{ mm}^2/\text{s}$ ($P < 0.001$)	[38]
DWI of the middle cerebellar peduncle and rostral pons to differentiate between patients with MSA-P, PSP,	The optimal cut-off level to discriminate patients with MSA-P from patients with PSP was a middle cerebellar peduncle rADC of $\geq 0.733 \times 10^{-3} \text{ mm}^2/\text{s}$ (sensitivity = 91%,	Increased rADC in the middle cerebellar peduncle and rostral pons in patients with MSA-P compared with patients with PSP or PD. Pons (caudal): Patients with PSP rADC = $0.785 \pm 0.090 \times 10^{-3} \text{ mm}^2/\text{s}$	[39]

Technique and region	Diffusion MRI findings	Key diffusion measures	Reference
or PD (caudal and rostral)	specificity = 84%). ADC measurements may have been utilized as surrogate markers in trials of disease-modifying medications [38].	Patients with MSA $rADC = 0.845 \pm 0.133 \times 10^{-3} \text{ mm}^2/\text{s}$ Patients with PD $rADC = 0.771 \pm 0.101 \times 10^{-3} \text{ mm}^2/\text{s}$ Healthy controls $rADC = 0.763 \pm 0.079 \times 10^{-3} \text{ mm}^2/\text{s}$ Pons (rostral): Patients with PSP $rADC = 0.745 \pm 0.110 \times 10^{-3} \text{ mm}^2/\text{s}$	
DWI of the putamen and SCP	Significantly higher SCP ADC in patients with PSP compared with patients with CBS or PD and healthy controls. The median ADC in the higher-valued hemisphere was significantly increased in patients with CBS. The hemispheric symmetry ratio in patients with CBS was lower than in patients with RS or PD and healthy controls.	Putaminal ADC provides good discrimination between patients with PD and patients with APD (RS and CBS). Patients with CBS $0.77 (0.75-0.79) \times 10^{-3} \text{ mm}^2/\text{s}$ Patients with RS $0.75 (0.74-0.79) \times 10^{-3} \text{ mm}^2/\text{s}$ Patients with PD $0.72 (0.71-0.73) \times 10^{-3} \text{ mm}^2/\text{s}$ Healthy controls $0.70 (0.69-0.71) \times 10^{-3} \text{ mm}^2/\text{s}$	[35]
DTI of the pons, cerebellum, and putamen to differentiate between patients with MSA-P and patients with PD.	FA and ADC detected early pathological involvement prior to magnetic resonance signal changes in patients with MSA-P. Early FA reduction and ADC increase are likely to be associated with subtle early degenerative processes in patients with MSA-P.	Increased ADC in the pons, cerebellum, and putamen, and reduced FA in patients with MSA compared with patients with PD and healthy controls. FA Pons = 0.38 Cerebellum = 0.30 Putamen = 0.35 ADC Pons = $0.98 \times 10^{-3} \text{ mm}^2/\text{s}$ Cerebellum = $0.96 \times 10^{-3} \text{ mm}^2/\text{s}$ Putamen = $0.83 \times 10^{-3} \text{ mm}^2/\text{s}$ Sensitivity and specificity of FA: 70.0% and 100.0% in the pons; 70.0% and 63.6% in the cerebellum; and 70.0% and 87.5% in the putamen.	[40]
DTI in patients with an implanted deep brain stimulation (DBS) device.	DTI is safe and delineation of the white matter pathway is feasible for patients with PD and an implanted DBS device.	The FA of the left SN was significantly lower than that of the right SN ($P < 0.05$ in both DBS-on and DBS-off states)	[41]
Dopamine transporter imaging	The neuromelanin value was significantly lower and the diffusion tensor values except FA were significantly higher in the RBD and PD groups than in the healthy group. Diffusion MRI detects nigrostriatal changes in RBD and early PD.	Neuromelanin/mean diffusivity value. Patients with RBD $SN_{pc} = 0.76/0.82$ Patients with PD $SN_{pc} = 0.83/0.80$	[42]

Technique and region	Diffusion MRI findings	Key diffusion measures	Reference
Conventional MRI DTI of the SN		The reduced volume of the SN in the patient with PD is attributable to iron deposition. FA was lower in the patient with PD than in the patient without PD (0.425 vs. 0.581), indicating a loss of neuronal integrity.	[43]
DTI of the SN and middle cerebellar peduncle.	FA was increased in all three subareas of the SN.	FA was increased in the three nigral subareas in patients with PD ($P < 0.01$). The right SN had higher FA than the left in all subareas ($P < 0.01$). The left middle cerebellar peduncle had increased FA ($P < 0.001$).	[44]
DWI of the putamen.	Putaminal diffusivity measurements to distinguish MSA-P from PD.	Prominent neuronal loss in the putamen; structural damage in the putamen would lead to enhanced diffusivity. Meta-analysis showed an overall sensitivity of 90% and specificity of 93%.	[29]
DTI of the rostral, middle and caudal SN and cerebral peduncle	Assessment of FA in the rostral, middle, and caudal regions of the SN. SN distinguishes early-stage <i>de novo</i> patients with PD from healthy controls.	Decreased FA in the caudal part of the substantial nigra with increased sensitivity and specificity even between individual subjects. Rostral region $t = 1.5; P = 0.12$ Middle region $t = 3.7; P = 0.001$ Caudal region $t = 11.9; P = 0.00001$	[20]
DTI of the SN	The FA is decreased in the nigrostriatal projection in parkinsonian patients, even during the early clinical stages	Decreased FA in the ROI along a line between the SN and the lower part of the putamen/caudate complex in patients with PD, even during the early clinical stages of the disease. FA in patients with PSP was decreased in most of the ROIs except for those in the neostriatum of parkinsonian patients showed a significant decrease in FA of the subthalamic ROI beside the SN. FA in the white matter of the premotor cortices was significantly smaller in patients with PSP or advanced PD compared with healthy controls.	[45]
DTI of the SN, red nucleus, and cerebral peduncle		FA was reduced in the rostral SN of subjects with early-stage PD.	[46]
DWI of the SN with increased iron (R2)		Reduction of FA inside the SN in patients with PD demonstrated a high correlation with an increase in iron.	[47]
DTI of the SN with increased iron (R2)	Differences between patients with PD and controls from voxel-based analysis of R2, mean	Reduction of FA inside the SN demonstrated a high correlation with an increase in iron in patients with PD.	[48]

Technique and region	Diffusion MRI findings	Key diffusion measures	Reference
	diffusivity, and FA maps [48].		
DTI of the SN		FA in the SN based on DTI was lower in patients with PD compared with healthy controls.	[49]
DTI of the SN		Decreased FA in the SN is associated with the increased motor in patients with PD.	[50]
DTI of the SN		Decreased FA in the SN is associated with the increase of motor symptoms in patients with PD.	[21]

Abbreviations: ADC: apparent diffusion coefficient; APD: atypical parkinsonism diseases; CBS: corticobasal syndrome; DBS: deep brain stimulation; DTI: diffusion tensor imaging; DWI: diffusion-weighted imaging; FA: fractional anisotropy; MSA: multiple system atrophy; MSA-P: multiple system atrophy with predominant parkinsonian features; PD: Parkinson's disease; PSP: progressive supranuclear palsy; rADC: regional apparent diffusion coefficient; RBD: rapid eye movement sleep behavior disorder; ROI: region of interest; RS: Richardson's syndrome; rTrace (D): regional trace (D); SCP: superior cerebellar peduncles; SN: substantia nigra; Unified Parkinson's Disease Rating Scale (UPDRS). AC: anterior commissure; CN: caudate nucleus; Ctr: age matched normal subjects as control; GP: globus pallidus; GPe: globus pallidus lateral segment; GPi: globus pallidus medial segment; PC: posterior commissure; PD12: Parkinson's disease in the early-stage group; PD345: Parkinson's disease in the advanced stage group. ROI: region of interest; SN: substantia nigra; SNc: substantia nigra pars compacta; SNr: substantia nigra pars reticulata; STN: subthalamic nucleus; VL: nucleus ventralis lateralis.

Table 3.
Biomarkers in the diagnosis of PD and APD.

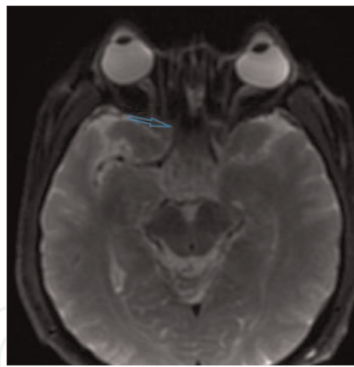


Figure 9.
DWI, 43-year-old patient PD, male (made by the authors).

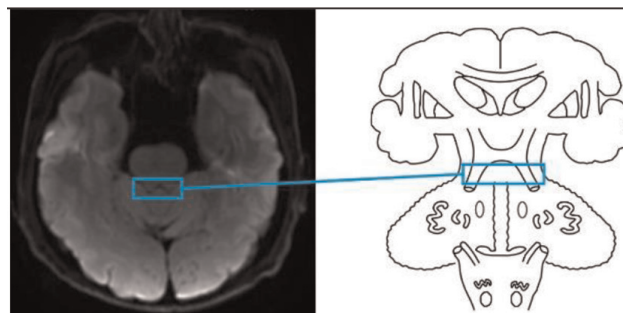


Figure 10.
Superior cerebellar peduncles (SCP) on the ROI map from 43-year-old patient PD, male. Adapted from results with interesting ROI (made by the authors).

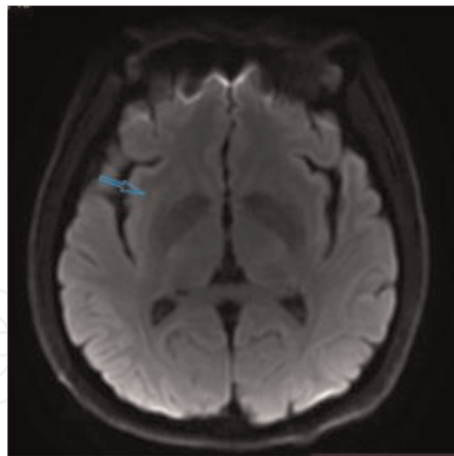


Figure 11.
Adapted from results with putaminal ROI from 43-year-old patient PD (made by the authors).

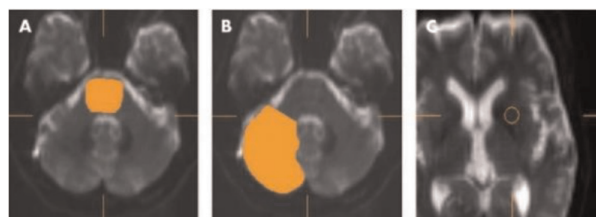


Figure 12.
ROIs in the pons (A), cerebellum (B), and putamen (C). Adapted from Ito et al. [40].

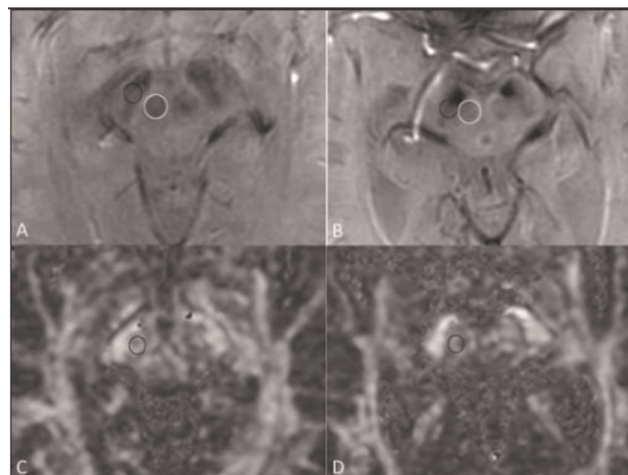


Figure 13.
DWI image in a 66-year-old-patient without PD (A), an axial slice of the midbrain shows a delineated SN (black circle), showing well-defined cleavage with the red nucleus (white circle). In a 68-year-old patient with PD (B), an axial slice of the midbrain on susceptibility-DWI shows a poorly delineated. Adapted from Oliveira et al. [43].

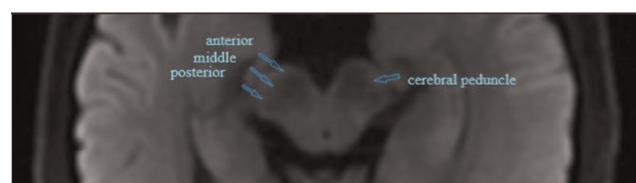


Figure 14.
Anterior, middle, and posterior SN in a 43-year-old patient PD (Adapted from results by the authors).

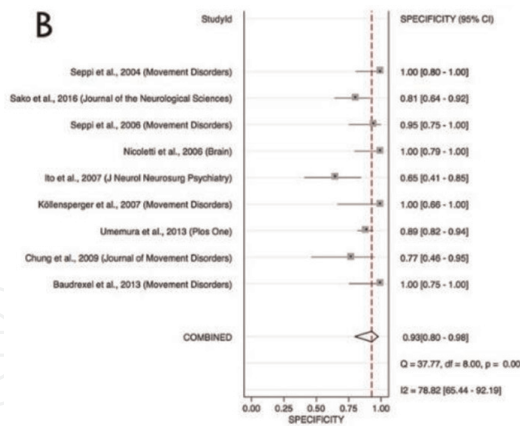


Figure 15. The overall specificity of putaminal diffusivity to discriminate MSA-P from PD. Adapted from Bajaj et al. [29].

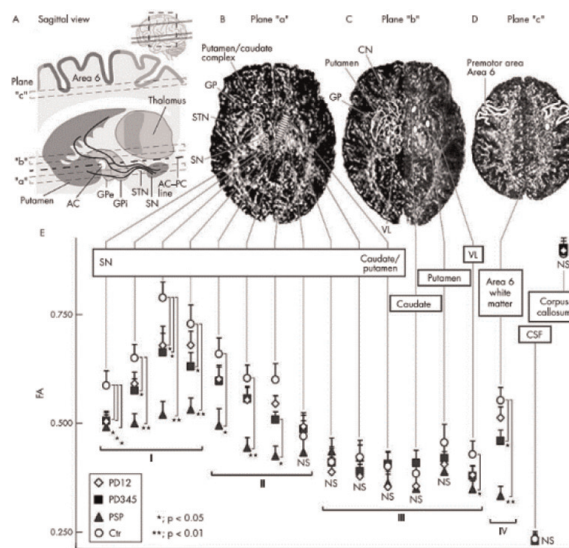


Figure 16. Anatomy of the extrapyramidal system in the paramedian sagittal view (A). Fibers of nigro-neostriatal projection, which are selectively lost in PD, are illustrated by black lines originating from the SN. FA images are derived from diffusion tensor images (B–D). FA in the extrapyramidal system of normal subjects and patients (E). Adapted from Ref. [45].

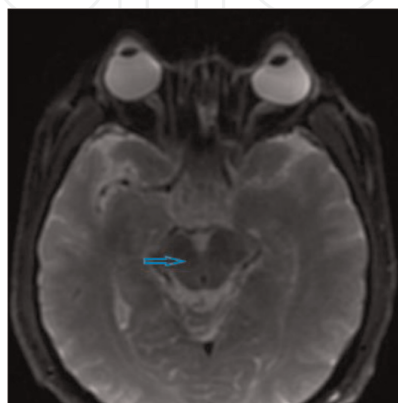


Figure 17. Axial sequences depicting the SN and red nucleus (blue arrow) from a 43-year-old patient PD (adapted by the authors).

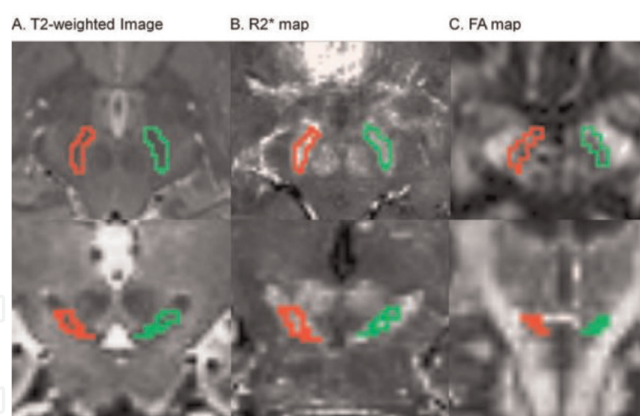


Figure 18. Image illustrating the location of the SN in T2-weighted images (A) and the co-registered ROIs on the R2* (B) and FA (C) maps on both axial (top row) and coronal (bottom row) sections. Adapted from Du et al. [47].

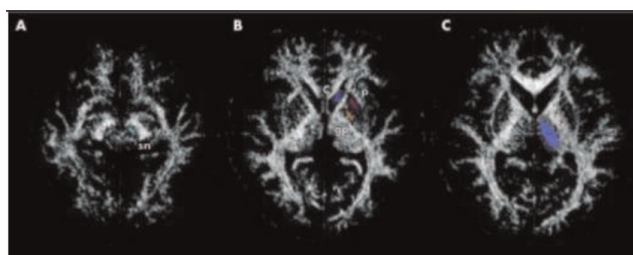


Figure 19. ROIs of gray matter structures: (A) substantia nigra (sn), (B) caudate (c), putamen (p), globus pallidus (gp), and (C) thalamus (t), drawn on axial diffusion tensor DTI images on the FA map. Adapted from Chan et al. [49].

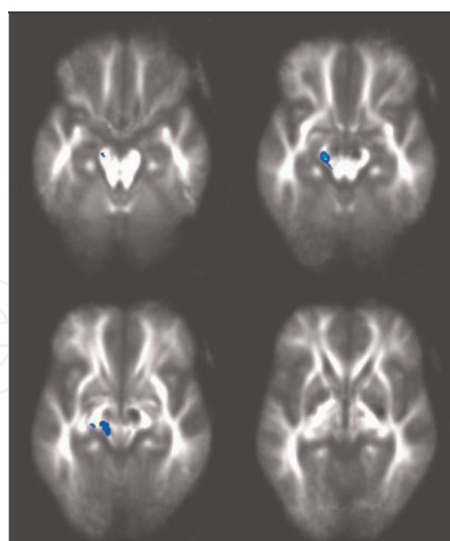


Figure 20. Significant voxel-wise correlations ($P < 0.05$, corrected) between decreased FA and increased total UPDRS scores were detected in the white matter at the level of the SN. Adapted from Zhan et al. [21].

4. Conclusion

Diffusion MRI, including isotropic and anisotropic techniques, has become increasingly important in the evaluation and diagnosis of patients with PD, and even

in other neurodegenerative diseases. The most common quantitative biomarkers are ADC and FA. Moreover, diffusion MRI has the advantages of being noninvasive, repeatable, and quantifiable, and has the ability to localize damage. It is likely that neuroimaging methods will become important research techniques in the area of biomarkers in future. In conclusion, the parameters estimated with diffusion MRI in patients with moderate-stage PD can distinguish between patients with PD or APD and healthy controls.

Acknowledgements

Greatly appreciated to the authors who allowed the use of the images as part of the construction of the chapter and to the Chinese Academy of Sciences for supporting this publication. It is necessary to clarify that the main author was affiliated with the Universidad Manuela Beltrán and the Universidad ECCI as a research professor, but it is published with the authors' own resources without any financial interest.

Conflict of interest

The authors declare no conflict of interest.

Author details

Gloria Cruz^{1*}, Shengdong Nie² and Juan Ramírez³


1 Faculty of Engineering, Department of Biomedical Engineering, Universidad ECCI, Bogotá, Colombia

2 Institute of Medical Imaging and Engineering School of Medical Instrument and Food Engineering, University of Shanghai for Science and Technology USST, Shanghai, China

3 Faculty of Engineering, Universidad Distrital Francisco José de Caldas, Bogotá, Colombia

*Address all correspondence to: g_milena@yahoo.com

IntechOpen

© 2023 The Author(s). Licensee IntechOpen. This chapter is distributed under the terms of the Creative Commons Attribution License (<http://creativecommons.org/licenses/by/3.0>), which permits unrestricted use, distribution, and reproduction in any medium, provided the original work is properly cited. 

References

- [1] Braak H, Rüb U, Gai W, et al. Idiopathic Parkinson's disease: Possible routes by which vulnerable neuronal types may be subject to neuroinvasion by an unknown pathogen. *Journal of Neural Transmission*. 2003;**110**:517-536
- [2] Hodaie M, Neimat J, Lozano A. The dopaminergic nigrostriatal system and Parkinson's disease: Molecular events in development, disease, and cell death, and new therapeutic strategies. *Neurosurgery*. 2007;**60**:17-28
- [3] Braak H, Del Tredici K, Rüb U, et al. Staging of brain pathology related to sporadic Parkinson's disease. *Neurobiology of Aging*. 2003;**24**:197-211
- [4] Deutschlander AB, Konno T, Soto-Beasley AI, et al. Association of MAPT subhaplotypes with clinical and demographic features in Parkinson's disease. *Annals of Clinical Translational Neurology*. 2020;**7**:1557-1563
- [5] Politis M. Neuroimaging in Parkinson disease: From research setting to clinical practice. *Nature Reviews. Neurology*. 2014;**10**:708-722
- [6] Anderson VC, Lenar DP, Quinn JF, et al. The blood-brain barrier and microvascular water exchange in alzheimer's disease. *Cardiovascular Psychiatry Neurology*. 2011;**2011**. DOI: 10.1155/2011/615829. [Epub ahead of print]
- [7] Dietrich O, Biffar A, Baur-Melnyk A, et al. Technical aspects of MR diffusion imaging of the body. *European Journal of Radiology*. 2010;**76**:314-322
- [8] Le Bihan D, Johansen-Berg H. Diffusion MRI at 25: Exploring brain tissue structure and function. *NeuroImage*. 2012;**61**:324-341
- [9] Stejskal EO, Tanner JE. Spin diffusion measurements: Spin echoes in the presence of a time-dependent field gradient. *The Journal of Chemical Physics*. 1965;**42**:288
- [10] Carr H, Purcell E. Effects of diffusion on free precession in nuclear magnetic resonance experiments. *Physics Review*. 1954;**94**:630-638
- [11] LeBihan D, Breton E, Lallemand D, et al. MR imaging of intravoxel incoherent motions: Application to diffusion and perfusion in neurologic disorders. *Radiology*. 1986;**161**:401-407
- [12] Warach S, Chien D, Li W, et al. Fast magnetic resonance diffusion-weighted imaging of acute human stroke. *Neurology*. 1992;**42**:1717-1723
- [13] Mitchell JG, Kogure K. Bacterial motility: Links to the environment and a driving force for microbial physics. *FEMS Microbiology Ecology*. 2006;**55**:3-16
- [14] Mori S. *Introduction to Diffusion Tensor Imaging*. Elsevier; 2007. DOI: 10.1016/B978-044452828-5/50017-X
- [15] Kon T, Mori F, Tanji K, et al. An autopsy case of preclinical multiple system atrophy (MSA-C). *Neuropathology*. 2013;**33**:667-672
- [16] Jones DK. *Diffusion MRI: Theory, Methods, and Applications*. DOI: 10.1093/med/9780195369779.001.0001
- [17] Chilla GS, Tan CH, Xu C, et al. Diffusion weighted magnetic resonance imaging and its recent trend-a survey. *Quantitative Imaging in Medicine and Surgery*. 2015;**5**:407-422

- [18] Basser PJ, Mattiello J, LeBihan D. Estimation of the effective self-diffusion tensor from the NMR spin Echo. *Journal of Magnetic Resonance - Series B*. 1994; **103**:247-254
- [19] Hagmann P, Jonasson L, Maeder P, et al. Understanding diffusion MR imaging techniques: From scalar diffusion-weighted imaging to diffusion tensor imaging and beyond. *Radiographics*. Oct 2006; **26**. DOI: 10.1148/rg.26si065510. [Epub ahead of print]
- [20] Vaillancourt D, Spraker M, Prodoehl J, et al. High-resolution diffusion tensor imaging in the substantia nigra of de novo Parkinson disease. *Neurology*. 2009; **72**:1378-1384
- [21] Zhan W, Kang GA, Glass GA, et al. Regional alterations of brain microstructure in Parkinson's disease using diffusion tensor imaging. *Movement Disorders*. 2012; **27**:90-97
- [22] Niethammer M, Eidelberg D. Chapter five—Network imaging in parkinsonian and other movement disorders: Network dysfunction and clinical correlates. In: Politis M, editor. *Imaging in Movement Disorders: Imaging in Non-Parkinsonian Movement Disorders and Dementias*, Part 2. Academic Press; 2019. pp. 143-184
- [23] Sako W, Murakami N, Izumi Y, et al. The difference in putamen volume between MSA and PD: Evidence from a meta-analysis. *Parkinsonism & Related Disorders*. 2014; **20**:873-877
- [24] Lehericy S, Bensimon G, Vidailhet M. *Parkinsonian Syndromes*. Elsevier Inc; 2015. DOI: 10.1016/B978-0-12-397025-1.00088-9
- [25] Williams DR, de Silva R, Paviour DC, et al. Characteristics of two distinct clinical phenotypes in pathologically proven progressive supranuclear palsy: Richardson's syndrome and PSP-parkinsonism. *Brain*. 2005; **128**:1247-1258
- [26] Boelmans K, Bodammer NC, Suchorska B, et al. Diffusion tensor imaging of the corpus callosum differentiates corticobasal syndrome from Parkinson's disease. *Parkinson Related Disorders*. 2010; **16**:498-502
- [27] Barsottini OGP, Felício AC, de Aquino CC, et al. Progressive supranuclear palsy: New concepts. *Arquivos de Neuro-Psiquiatria*. 2010; **68**:938-946
- [28] Mascalchi M, Vella A, Ceravolo R. Movement disorders: Role of imaging in diagnosis. *Journal of Magnetic Resonance Imaging*. 2012; **35**:239-256
- [29] Bajaj S, Krismer F, Palma J-A, et al. Diffusion-weighted MRI distinguishes Parkinson disease from the parkinsonian variant of multiple system atrophy: A systematic review and meta-analysis. *PLoS One*. 2017; **12**:e0189897
- [30] Scherfler C, Schocke MF, Seppi K, et al. Voxel-wise analysis of diffusion weighted imaging reveals disruption of the olfactory tract in Parkinson's disease. *Brain*. 2006; **129**:538-542
- [31] Sobhani S, Rahmani F, Aarabi MH, et al. Exploring white matter microstructure and olfaction dysfunction in early Parkinson disease: Diffusion MRI reveals new insight. *Brain Imaging and Behavior*. 2019; **13**:210-219
- [32] Schocke M, Seppi K, Esterhammer R, et al. Diffusion-weighted MRI differentiates the Parkinson variant of multiple system atrophy from PD. *Neurology*. 2002; **58**:575-580
- [33] Schocke M, Seppi K, Esterhammer R, et al. Trace of diffusion tensor differentiates the Parkinson variant of

multiple system atrophy and Parkinson's disease. *NeuroImage*. 2004;**21**:1443-1451

[34] Nicoletti G, Tonon C, Lodi R, et al. Apparent diffusion coefficient of the superior cerebellar peduncle differentiates progressive supranuclear palsy from Parkinson's disease. *Movement Disorders*. 2008;**23**:2370-2376

[35] Rizzo G, Martinelli P, Manners D, et al. Diffusion-weighted brain imaging study of patients with clinical diagnosis of corticobasal degeneration, progressive supranuclear palsy and Parkinson's disease. *Brain*. 2008;**131**:2690-2700

[36] Seppi K, Schocke M, Mair KJ, et al. Progression of putaminal degeneration in multiple system atrophy: A serial diffusion MR study. *NeuroImage*. 2006;**31**:240-245

[37] Nicoletti G, Fera F, Condino F, et al. Imaging of middle cerebellar peduncle width: Differentiation of multiple system atrophy from pure: Methods: Results: Conclusion. *Radiology*. 2006;**239**:825-830

[38] Paviour D, Thornton J, Lees A, et al. Diffusion-weighted magnetic resonance imaging differentiates parkinsonian variant of multiple-system atrophy from progressive supranuclear palsy. *Movement Disorders*. 2007;**22**:68-74

[39] Seppi K, Schocke MF, Prenschiuetz-Schuetzenau K, Mair K, et al. Topography of putaminal degeneration in multiple system atrophy: A diffusion magnetic resonance study. *Movement Disorders*. 2006;**21**:847-865

[40] Ito M, Watanabe H, Kawai Y, et al. Usefulness of combined fractional anisotropy and apparent diffusion coefficient values for detection of involvement in multiple system atrophy. *Journal of Neurology, Neurosurgery, and Psychiatry*. 2007;**78**:722-728

[41] Li Y, He N, Zhang C, et al. Mapping motor pathways in Parkinson's disease patients with subthalamic deep brain stimulator: A diffusion MRI Tractography study. *Neurological Therapy*. 2022:659-677

[42] Takahashi H, Kashiwagi N, Arisawa A, et al. Imaging of the nigrostriatal system for evaluating the preclinical phase of Parkinson's disease development: The utility of neuromelanin, diffusion MRI, and DAT-SPECT. *The British Journal of Radiology*. 2022;**95**:40-41

[43] de Oliveira RV, Pereira JS. The role of diffusion magnetic resonance imaging in Parkinson's disease and in the differential diagnosis with atypical parkinsonism. *Radiologia Brasileira*. 2017;**50**:250-257

[44] Lenfeldt N, Larsson A, Nyberg L, et al. Fractional anisotropy in the substantia nigra in Parkinson's disease: A complex picture. *European Journal of Neurology*. 2015;**22**:1408-1414

[45] Yoshikawa K. Early pathological changes in the parkinsonian brain demonstrated by diffusion tensor MRI. *Journal of Neurology, Neurosurgery, and Psychiatry*. 2004;**75**:481-484

[46] Modrego PJ, Fayed N, Artal J, et al. Correlation of findings in advanced MRI techniques with global severity scales in patients with Parkinson disease. *Academic Radiology*. 2011;**18**:235-241

[47] Du G, Lewis MM, Styner M, et al. Combined R2* and diffusion tensor imaging changes in the substantia nigra in Parkinson's disease. *Movement Disorders*. 2011;**26**:1627-1632

[48] Péran P, Cherubini A, Assogna F, et al. Magnetic resonance imaging markers

of Parkinson's disease nigrostriatal signature. *Brain*. 2010;**133**:3423-3433

[49] Chan L-L, Rumpel H, Yap K, et al. Case control study of diffusion tensor imaging in Parkinson's disease. *Journal of Neurology, Neurosurgery, and Psychiatry*. 2007;**78**:1383-1386

[50] Prakash BD, Sitoh Y-Y, Tan LCS, et al. Asymmetrical diffusion tensor imaging indices of the rostral substantia nigra in Parkinson's disease. *Parkinsonism & Related Disorders*. 2012; **18**:1029-1033

[51] Seppi K, Schocke MFH, Donnemiller E, Esterhammer R, Kremser C, Scherfler C, et al. Comparison of diffusion-weighted imaging and [123I]IBZM-SPECT for the differentiation of patients with the Parkinson variant of multiple system atrophy from those with Parkinson's disease. *Movement Disorders*. 2004;**19**:1438-1445

[52] Paviour D, Price S, Stevens J, et al. Quantitative MRI measurement of superior cerebellar peduncle in progressive supranuclear palsy. *Neurology*. 2005;**64**:675-679

[53] Nicoletti G, Fera F, Condino F, et al. MR imaging of middle cerebellar peduncle width: Differentiation of multiple system atrophy from Parkinson disease. *Radiology*. 2006;**239**:825-830